International Journal of Advances in Scientific Research and Engineering (ijasre)

E-ISSN : 2454-8006

DOI: 10.31695/IJASRE.2022.8.11.3

Volume 8, Issue 11
November - 2022

Effect of Dust Accumulation on the Performances of Solar Panels in Static and Tracking Systems in Bauchi Metropolis of Nigeria

ADAMU A. A.[1], ADAMU K. S.[2], MOHAMMED A.[3], SULE M.A.[4], IBRAHIM U.S.[5]

[1]Dept. Of Mechanical Engineering Technology, Abubakar Tatari Ali Polytechnic, Bauchi, Nigeria

[2,5] Dept. Of Electrical Engineering Technology, Federal Polytechnic Kaltungo, Gombe, Nigeria

[3] Niger-Delta Power Holding Company Limited, Kogi, Nigeria

[4]Dept. Of Computer Engineering Technology, Federal Polytechnic Kaltungo, Gombe, Nigeria

ABSTRACT

The research aimed at comparing the effect of dust accumulation on the performances of solar PV modules in static position and on a tracking system within Bauchi metropolis of Nigeria $(10.3060°N, 9.8404°E)$*, during the harmattan season – November to December. Dust deposition on the surface of PV panel reduces the conversion efficiency by absorbing and preventing the Solar radiation from reaching the cells of the panel. This necessitated the need to develop a reliable tool to relate energy production from solar cells with respect to dust deposition on both static and solar tracking PV modules. A test bed was designed for the field measurement of output current, voltage, temperature and dust weight data from the two PV modules." Centsys" polycrystalline solar panels* $(12V, 60W)$ *was used for the research. A statistical technique involving regression analysis in SPSS software was used to correlate between the various measured data from the test bed to predict the effect of dust accumulation on the surface of each module, which will enable solar power installers to take necessary measures for improving the PV module's conversion efficiency during the period under review. The research result showed that the effect of dust on the tracking solar PV module is less significant compared to the static panel, giving the former a better conversion efficiency.*

Keywords: Solar Tracker, Photovoltaic (PV) Module, Irradiance, Short Circuit Current, Open Circuit Voltage.

1. INTRODUCTION

During the last three decades, the demand for non-conventional energy resources has increased in generating electricity due to limited and cost of conventional resources such as fossil fuel and hydro-power generation [1]. Renewable energy emerges as an alternative to conventional energy resources for the production of clean energy [2]. Among the renewable energy resources, solar energy is the permanent and abundant energy source. The availability of this alternative source of energy offers a strategic solution to power supply problems [3]. It is important to implement the photovoltaic system technology suitable for the relevant locations in order to take into consideration the local environment aspects and optimize the energy yield [4].

However, one of the constraints of photovoltaic (PV) systems, especially in Africa, is related to dust deposition on the photovoltaic modules surface. The accumulation of dust particles on the surface of PV module greatly affects its performance [5]. Therefore, the performance of PV modules could be divided into two categories, namely the geographical factors which include longitude, latitude, and solar intensity, and the environmental factors, such as temperature, wind, humidity, pollution, dust, rain, *etc*. and also the type of PV technology used [6]. From the previous researches, it could be concluded that PV modules have particular behavior in specific climate conditions.

The rating of solar PV module is carried out in the industry under Standard Test Conditions (STC) with the solar cell temperature at 25 ℃, solar irradiance of 1000 W/m^2 and the atmospheric air mass fixed at 1.5 (Ahmed *et al.* 2013). These conditions can be achieved easily at the industry, but they are not practically obtainable outdoor due to the aforementioned factors.

Dust accumulation on solar photovoltaic (PV) modules is a natural phenomenon since the solar panels are usually installed outdoor. The power output delivered from a photovoltaic (PV) module depends on its temperature as well as the amount of solar irradiance reaching the solar cells [7]. Meanwhile, dust particles deposit is mostly responsible for limiting the amount of sun

radiation reaching the solar cells and consequently the cell temperature [8]. Dust particles deposited on PV cells absorb and block the solar radiation, thereby reducing the solar energy reaching the solar cells [9].

The accumulation of dust and other output power reduction factors on a static PV module, such as bird droppings and mud tend to be responsible for up to 30% to 40% of the panel's power losses **(**Prasanthi & Jayamadhuri, 2015**)**. Rays from the sun strike a PV module at an angle θ. Suppose the sun rays strike at a fixed intensity (λ), then the available sun energy to the solar cell for power generation (P) can be calculated as in Equation (1).

$$P = A\lambda Cos\theta \quad \ldots(1)$$

Where, A is the limiting conversion factor, since not all the sunrays incident on the panel can be converted into electrical energy. Hence, maximum power will generate only when θ = 0, i.e. the Sunlight hits the PV cells along the normal. When the sunlight falls on the panel at an angle other than 90 degrees, less power will be generated [10]. If the panel is static, there will be considerable power loss during the day. This is due to the daily movement of the sun as the earth rotates on its orbit. Due to constant changing of the sun's direction, the value of θ changes continuously. The power loss will be there for non-zero value of θ. Hence the angle of stationary panel should be at optimum position where the panel can generate maximum power (Sharma et al. 2020). Figure 1 shows the angle of incidence of the sunrays to the solar panel.

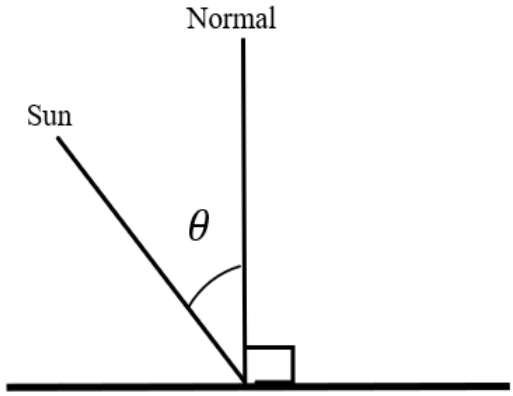

Fig. 1: Angle of Incidence of the Sun to the Normal

When a dust particle settles on the solar PV module, the incident angle is denoted by θ, as shown in Figure 2. When θ is not equal to zero, the shadow of the dust particle is oval is shape (Wang et al. 2017).

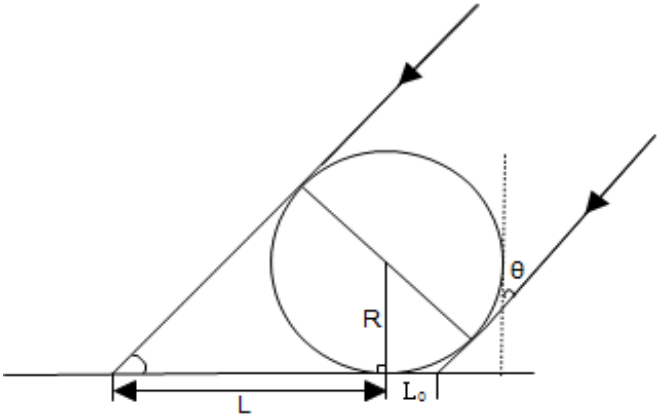

Figure 2: Incident Angle with Dust Particle on horizontal Panel

Where $L + L_o$ and R are the *major* and *minor* of axes respectively.

It is obvious that a tracking solar panel dislodges the deposition of dust settled on its surface, as it constantly moves in the direction of the sunlight (Wang et al. 2017). Figure 3 shows the incident ray on a panel with dust particle, when the module is inclined at an angle to the horizontal.

DOI: 10.31695/IJASRE.2022.8.11.3

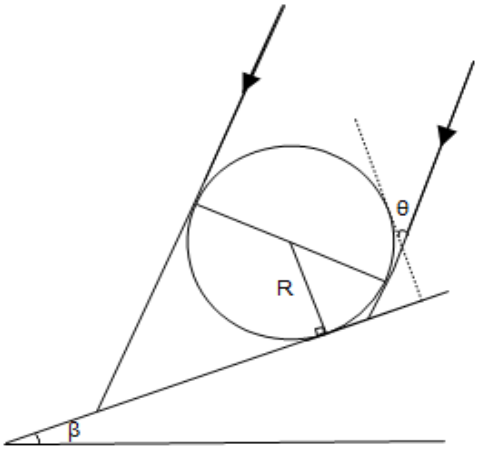

Figure 3: Incident Angle with Dust Particle on an inclined Panel

In view of the foregoing, it can be concluded that, the effect of dust deposit on static solar panel may not be the same as in a tracking solar PV module because the accumulation of dust could be lesser in the case of the latter, due to its moving nature, which may shed some of the dust off the PV module. Therefore, the outcome of the research will help in making choice when installing a solar PV module in order to maximize the output power generation. The research is significantly important for PV module installations, especially in African continent and some part of the globe experiencing dusty weather conditions.

- The primary objectives of this study is to evaluate the effect of dust accumulation on the performances of solar panels in static and tracking systems.
- The study was conducted in Bauchi metropolis of Nigeria.
- A statistical technique involving regression analysis in SPSS software was used to analyse the test results.
- The effect of dust on the tracking solar PV module was found to be less significant compared to the static panel, giving the former a better conversion efficiency.

2. METHODOLOGY

2.1 Data Acquisition Setup

The experimental photovoltaic module used in this research is the CENTSYS solar panel having maximum voltage rating of 18.20 V, maximum power rating of 60 $Watts$ and a dimension of 63.0cm * 67.0cm*3cm and is fabricated using polycrystalline silicon technology. One photovoltaic module was fixedly-orientated at an optimally-determined inclination angle facing Southward for maximum solar energy harvest and the other mounted on a solar tracking system using horizontal single axis solar tracking, at a location devoid of overcasts from nearby trees and buildings.

The schematic representation of the experimental setup is shown in Figure 4, with all pertinent equipment clearly labeled. The measuring equipment used are listed as follows:

1. Two identical 60 watts polycrystalline solar modules
2. Two digital multi-meters
3. Digital weighing balance
4. 150watts/100Ω Rheostat
5. Infrared digital thermometers

DOI: 10.31695/IJASRE.2022.8.11.3

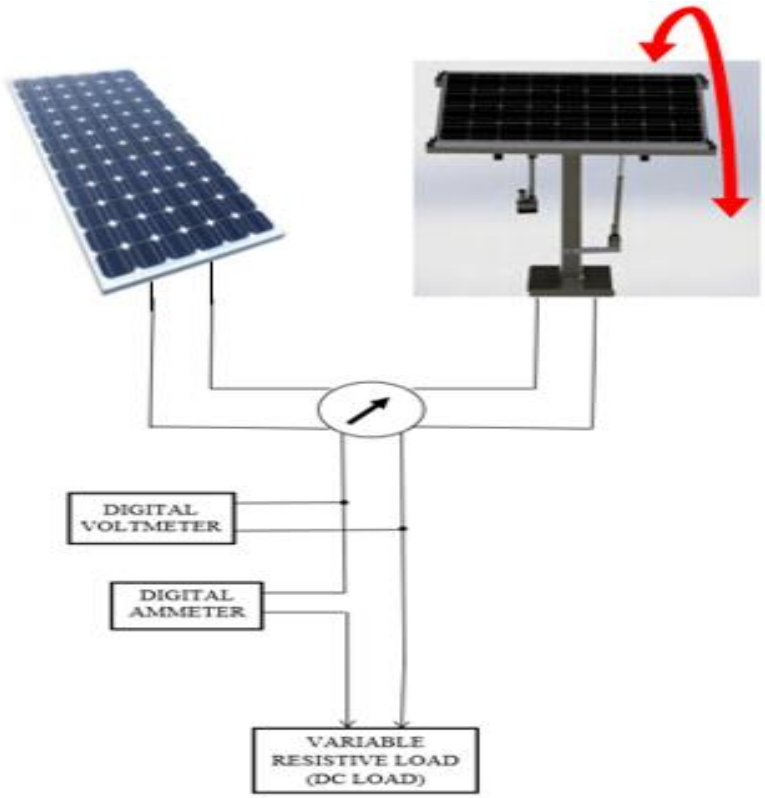

Figure 4: Data Acquisition Setup

2.2 PV Module Data Acquisition Framework

The field data acquisition scope encompasses hourly cell temperature, module current, module voltage and quantitative dust measurements. The flow chart depicted in Figure 5 constitute the experimental procedure with which to create the necessary current-voltage and power-voltage database on the experimental PV module.

DOI: 10.31695/IJASRE.2022.8.11.3

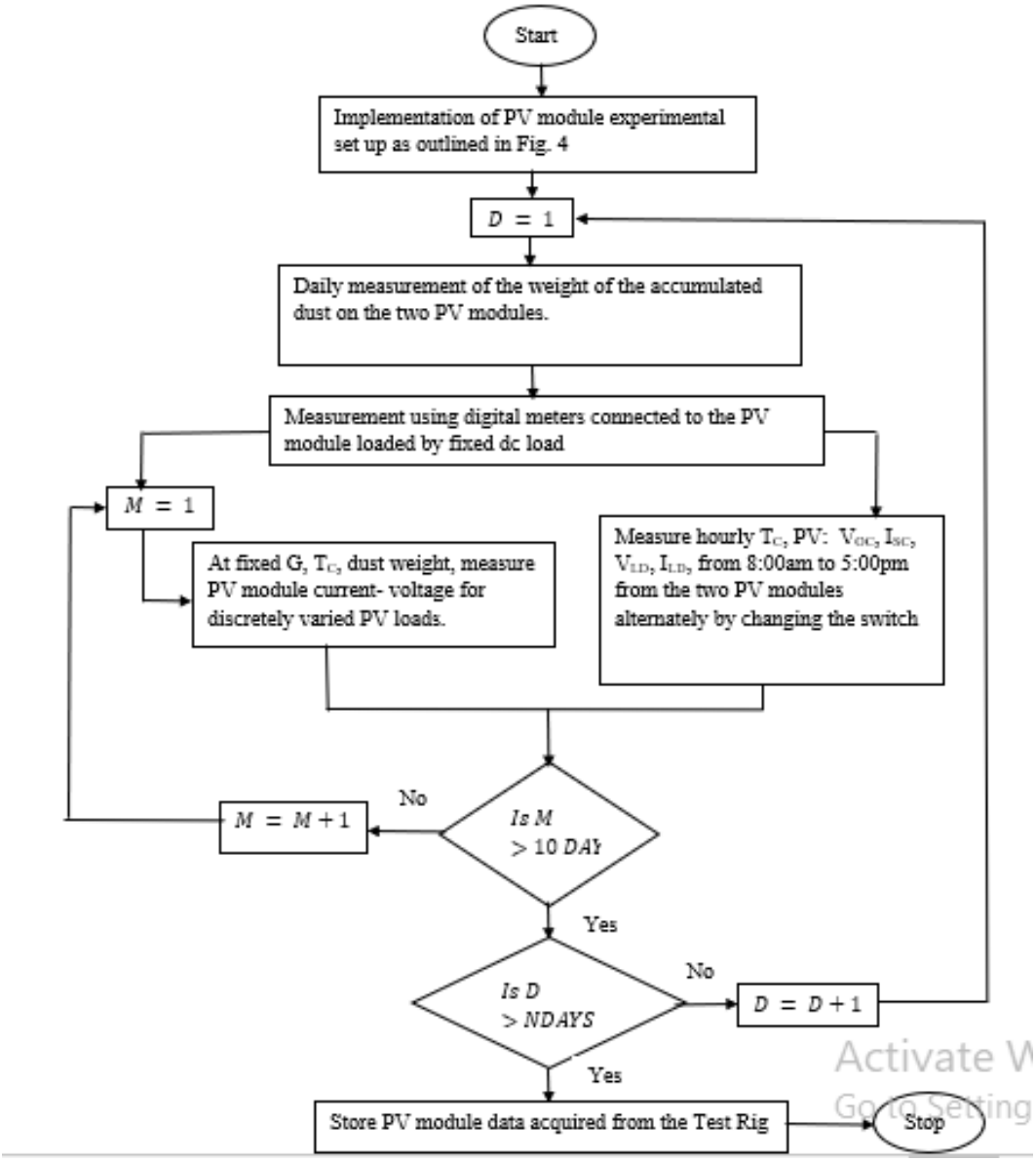

Figure 5: Experimental PV module Data Acquisition Framework

2.3 Solar Cell Model

A mathematical description of current-voltage terminal characteristics for PV cells is available in literature. The single exponential equation which models a PV cell is derived from the physics of the PN junction (diode) and is generally accepted as reflecting the characteristic behaviour of the cell. A solar cell is usually represented by an electrical equivalent one-diode model as shown in Figure 6

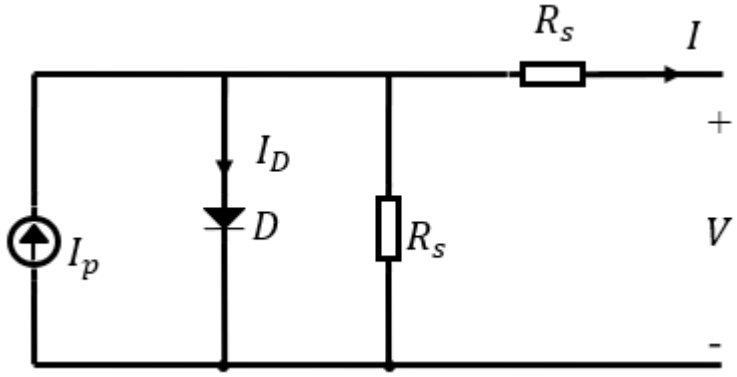

Figure 6: Equivalent PV Cell Circuit

The voltage-current characteristic equations of a solar cell as given by Tsai *et al*. (2008) are presented in Equations (2) to (5).

DOI: 10.31695/IJASRE.2022.8.11.3

$$I = I_{ph} - I_s\left[exp\frac{q(V+IR_s)}{AkT_c} - 1\right] - (V + IR_s)/R_{sh} \quad \ldots(2)$$

Where I_{ph} is the light-generated current or photocurrent;

$I_s$is the saturation current of diode.

$$I_{ph} = [I_{sc} + K_i(T_c - T_{Ref})]G_a \quad \ldots(3)$$

Where I_{sc} is the cell's short-circuit current at 25℃ and 1kW/m^2.

$G_a$is the solar irradiation in W/m^2.

$$I_s = I_{rs}(\frac{T_c}{T_{Ref}})^3 \exp[q(\frac{E_G\left(\frac{1}{T_{Ref}} - \frac{1}{T_c}\right)}{kA}] \quad \ldots(4)$$

Where I_{rs} is the reverse saturation current of the diode at a reference temperature T_{Ref} and a solar radiation, E_G is the band-gap energy of the semiconductor used in the cell.

$$\text{And } I_{rs} = I_{sc}/[\exp\left(\frac{qV_{oc}}{N_s kAT_c}\right) - 1] \quad \ldots(5)$$

Equations (2) to (5) were used in building the Simulink model of the solar cell.

The performance of different PV modules is measured at a standard test condition (STC), which is defined in Table 1 (Nema *et al.*, 2010).

Table 1: STC Parameters for PV Module

Parameter	
Cell temperature, T_c	25° C
Global solar irradiance, G_a	1000 W/m^2
Air mass, A	1.5

2.4 Solar Tracking PV Module

The design of the solar tracker was oriented to adopt the horizontal single-axis rotation (moving from East to West), meaning that the servomotor was mounted such that the tracker adopts a single-axis freedom of movement.

The solar tracker components comprise of the solar PV module, a charge controller and lead-acid batteries. While the control circuit comprises of other components such as the light-dependent resistor (LDR) sensors, voltage regulator unit, and ATMEGA328 microcontroller unit. The sun's intensity is sensed by one of the LDR sensors which sends its signal to the microcontroller. The microcontroller, having received the LDR's signal actuates the servomotor, which rotates the PV module. The electrical power generated by the PV module is stored in the lead-acid battery and is used to power the various solar tracking components. The solar PV module's positioning algorithm is depicted in Figure 7.

DOI: 10.31695/IJASRE.2022.8.11.3

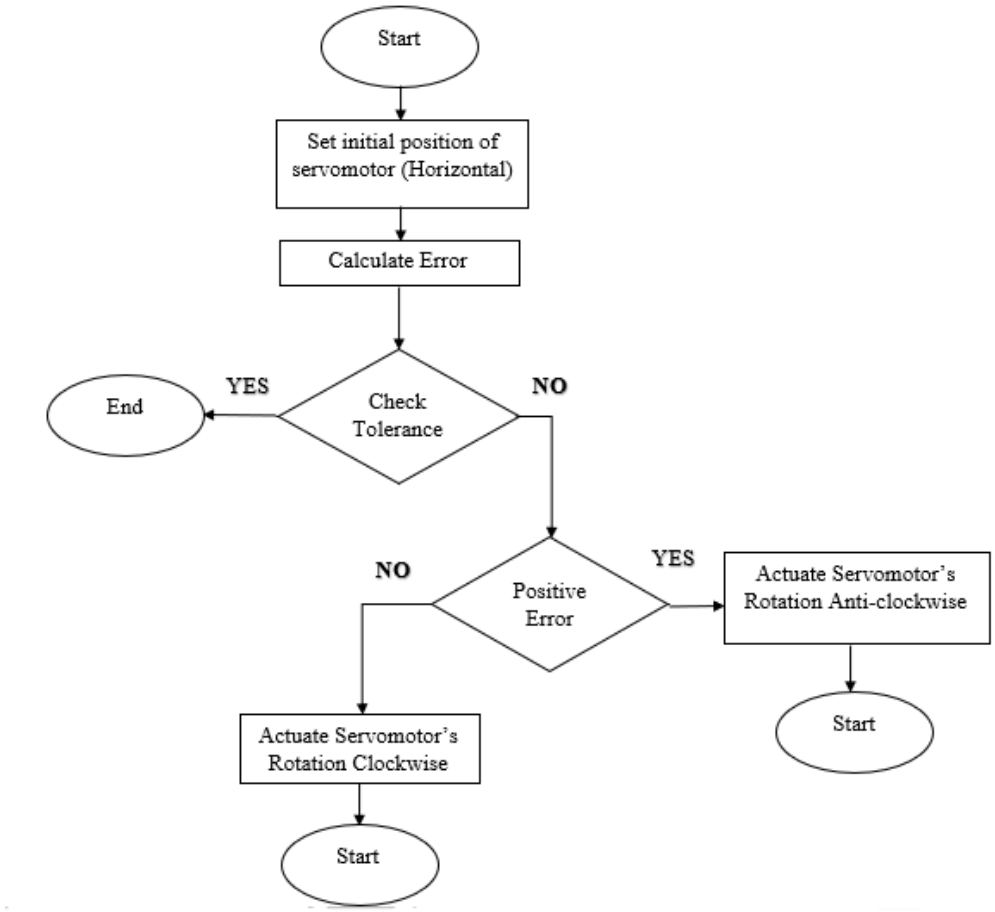

Figure 7: Flowchart of the Solar PV Module's Rotation Algorithm

2.5 Data Base for Dust Weight/Current-Voltage Values and I-V Curve Data Trace

In order to create the database for the accumulated dust weight values on the modules, the two modules are cleaned and a leather material that is exactly the size of the area of the cells on the panels is cut and placed on the PV modules. The leather material is removed to get the average weight of dust deposition on each PV module at the end of each day.

Solar irradiance, Temperature, current voltage data for the PV modules were measured for a period of 21 days by Connecting the PV modules to a 150 watts/100Ω Rheostat. A voltmeter was connected across a module to measure its terminal voltage. An ammeter was also connected in series with the module to measure its load current. The rheostat was kept at fixed resistance, i.e. mid-point. and the current-voltage values were recorded. The direction of the switch was then changed to measure the current and voltage from the other module. These procedures were repeated at hourly intervals from 8:00am – 5:00pm for 21 days.

To generate the data for I-V and P-V curves, the modules were connected as in Figure 4. At a particular G, T_{Cell} and dust weight, the rheostat was varied from minimum to maximum values in step and the corresponding current and voltage values were recorded from the two modules alternately by changing the switch. The procedure was repeated for various dust weight values at a fixed G and T_{Cell}.

2.6 Statistical Data Analysis

Firstly, the field data gathered were checked for incomplete data, and then keyed into SPSS data editor. The data were checked for missing values, outliers, normality, and multi-collinearity. Demographic characteristics of the data was obtained through descriptive statistics. The analysis was concluded using multiple regression to predict the power outputs of the PV modules from the variables namely, solar irradiance, temperature and dust weight. In order to perform the regression analysis, the following procedures are adopted herein.

i. Paired sample t-test was conducted to evaluate the impact of dust accumulation on module's temperature. This aimed at checking whether there is significant difference in temperature when the module is either rotating or static.
ii. Correlation analysis was carried out to check the relationship between the dependent variables; Power delivered to the load (P_L), Load voltage (V_L), Load current (I_L) Short circuit current (I_{SC}) and open circuit voltage (V_{OC}) and the independent variables; Irradiance (G) and Dust weight (D).

DOI: 10.31695/IJASRE.2022.8.11.3

iii. Multiple regression analysis was carried out against the two independent variables Irradiance (*G*) and dust weight (*D*).

3. RESULTS AND DISCUSSION

The solar irradiance and the PV temperature measurements were recorded and plotted against time of the day (hours) in Excel environment as shown in Figures 8 and 9 respectively. Similarly, comprehensive statistical characterizations of the solar irradiance with temperature change and dust deposit with average power losses are summarized in Tables 2 to respectively. Table 5 depicts the extracted values of current, voltage and maximum power delivered to the load.

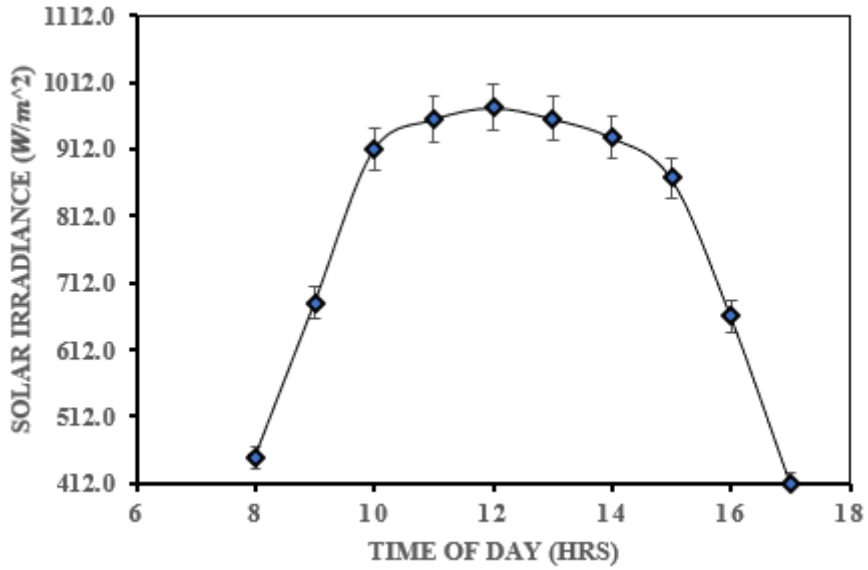

Figure 8: Plot of Solar Irradiance versus Time of Day

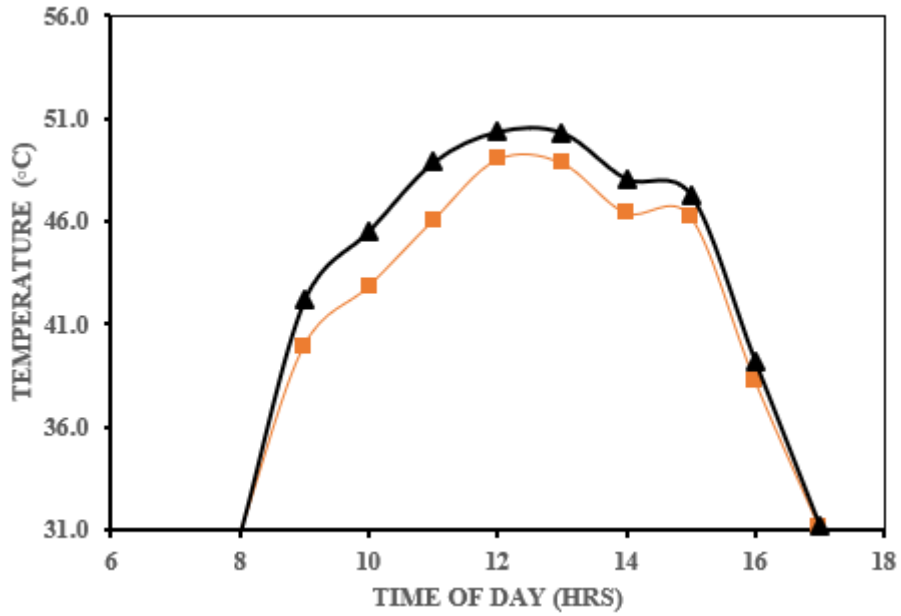

Figure 9: Plot of PV Module Temperature versus Time of Day

DOI: 10.31695/IJASRE.2022.8.11.3

Table 2: Summary of Statistical Characterization of Solar Irradiance and Temperature Observed at the Experimental Site

Statistical Information	Solar Irradiance (W/m^2)	Module Temperature (Tracking) T_CA (℃)	Module Temperature (Static) T_CB (℃)
Maximum	1100	54.3	52.5
Average	781	43	42
Minimum	172	27	26
Median	878	47	45
Mode	988	31.4	45

Table 3: Average Daily Measured Temperature

Day	G (W/m^2)	T_CA (◦C)	T_CB (◦C)
1	728	41.6	41.0
2	723	45.2	44.7
3	725	45.5	44.8
4	788	42.5	41.2
5	746	44.8	43.3
6	835	46.4	45.8
7	841	46.4	45.2
8	803	42.9	42.2
9	757	41.8	41.3
10	785	45.9	44.6
11	811	46.7	46.0
12	818	42.9	42.2
13	829	47.5	46.1
14	755	42.7	42.5
15	853	47.4	46.0
16	796	43.0	42.0
17	752	42.5	41.0
18	766	44.2	43.5
19	728	40.6	40.6
20	716	41.8	41.0
21	843	46.9	46.1

The measured I-V and P-V relationship are respectively depicted in Figures 10 and 11 for each dust accumulation level, while solar irradiance and temperature were held at the experimentally determine average value.

DOI: 10.31695/IJASRE.2022.8.11.3

Table 4: Average Daily Measured Data from the Experimental Test Bed

Day	G (W/m^2)	Dust Panel A (Tracker) (g/m^2)	Dust Panel B (Static) (g/m^2)	Panel A V_L(A) (V)	Panel A I_L(A) (A)	Panel B V_L(B) (V)	Panel B I_L(B) (A)	$P_L(A)$ (Tracker) (Watts)	P_L(B) (Static) (Watts)
1	728	5.5	5.6	15.2265	2.5255	13.2445	2.2742	53.9126	51.1102
2	723	5.8	6.4	19.9424	2.4246	13.0824	2.1240	53.8532	51.1055
3	725	7.1	7.5	19.9543	3.8769	19.5608	3.7004	52.8932	50.5415
4	788	12.9	13.2	16.2150	2.2968	14.1524	2.1924	49.1543	47.0764
5	746	9.1	9.4	17.9147	1.0842	17.7521	0.9099	51.0776	50.0016
6	835	3.6	3.8	19.9854	4.1503	19.8538	4.0848	58.1230	57.2114
7	841	2.6	2.8	19.0613	2.5124	14.6424	2.6224	58.7546	57.4192
8	803	16.7	17.9	17.2035	2.6025	13.3146	2.0022	44.7981	43.3676
9	757	43.0	43.3	10.2253	0.7726	9.2656	0.7556	16.9430	15.1528
10	785	52.4	52.7	7.3862	0.7765	5.6436	0.7528	6.7993	5.2229
11	811	16.5	16.9	16.2625	2.1424	13.9364	1.9957	45.8910	45.7678
12	818	13.5	13.9	17.2879	2.5136	14.5930	2.0964	49.4015	47.9875
13	829	11.0	11.3	16.9702	2.3068	14.2642	2.2845	53.0987	52.1025
14	755	20.4	20.7	15.3372	2.8808	19.1046	2.7270	36.8951	35.0096
15	853	25.9	26.4	18.9586	1.9038	18.6619	1.7811	30.0012	29.6767
16	796	29.4	30.1	10.1534	1.3858	9.8135	1.3041	40.7094	39.4018
17	752	36.3	36.7	10.2265	0.8845	9.4235	0.8246	39.9934	37.7843
18	766	48.8	54.6	17.3833	0.4877	17.1185	0.4663	9.8754	7.04996
19	728	6.9	7.0	16.3878	2.7852	13.5142	2.1145	54.2778	52.5201
20	716	0.0	0.0	20.1558	2.8214	15.4458	2.3282	59.4873	58.1068
21	843	0.0	0.0	20.1453	4.6842	20.1184	4.6838	59.9605	59.4489

Table 5: Extracted Values of Current, Voltage and Maximum Power Delivered to the Load from the I-V Characteristic Curves

		T = 49.3℃, G = 988 W/m^2					
Dust Panel A (Tracking) (g/m^2)	Dust Panel B (Static) (g/m^2)	V_L(A) (V)	I_L(A) (A)	V_L(B) (V)	I_L(B) (A)	$P_L(A)$ (Tracking) (Watts)	P_L(B) (Static) (Watts)
48.8	54.6	17.3833	0.4877	17.1185	0.46631	9.8754	7.04996
43.0	43.3	17.9147	1.0842	17.7521	0.90997	16.9430	15.1528
25.9	26.4	18.9586	1.9038	18.6619	1.78111	30.0012	29.6767
20.4	20.7	15.3372	2.8808	19.1046	2.72709	36.8951	35.0096
7.1	7.5	19.9543	3.8769	19.5608	3.70041	52.8932	50.5415
3.6	3.8	19.9854	4.1503	19.8538	4.08484	58.1230	57.2114
0	0	20.1453	4.6842	20.1184	4.68389	59.9605	59.4489

DOI: 10.31695/IJASRE.2022.8.11.3

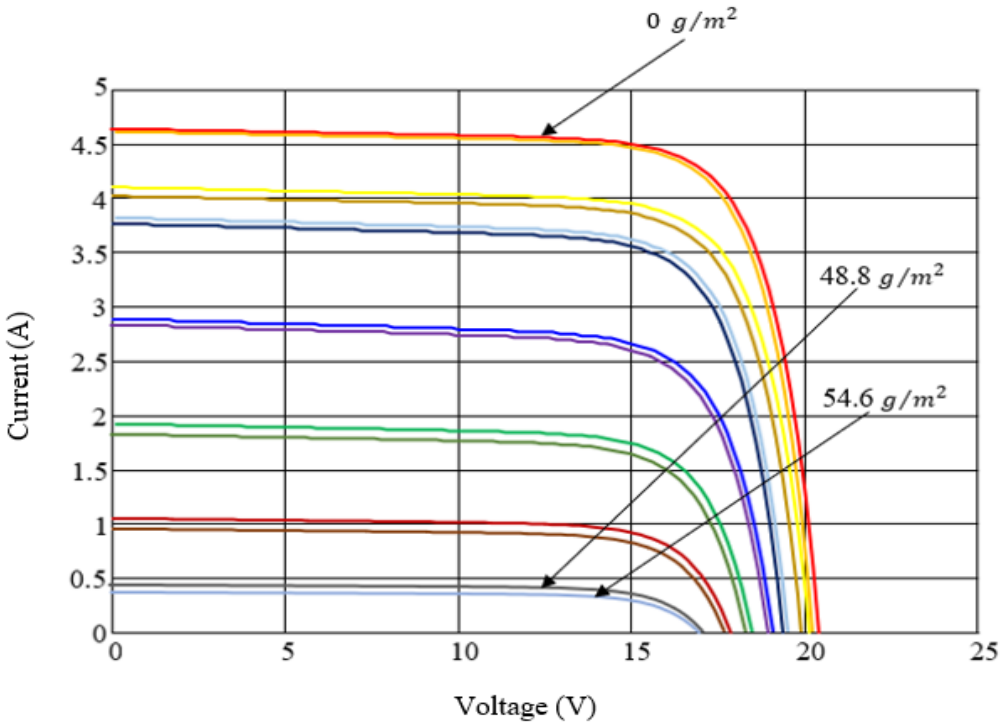

Figure 10: Measured I-V Characteristic Curves as a Function of Dust (T = 49.3℃, G = 988 W/m^2)

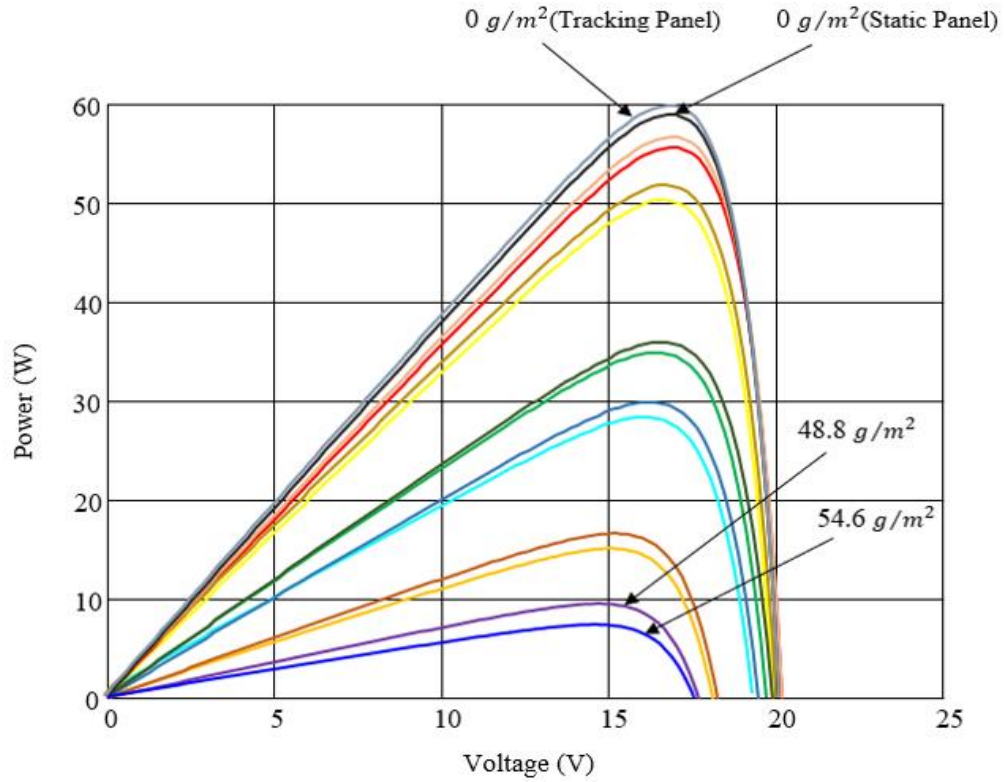

Figure 11: Measured P-V Characteristic Curves as a Function of Dust (T = 49.3℃, G = 988 W/m^2)

Result of Regression and Correlation Analysis

The overall goal of this research segment has been on the development of statistical analytical model and meta-heuristic technique based on field measurement that could accurately predict the operational performance of an experimental PV module when subjected to dust accumulation on the surface of the module.

DOI: 10.31695/IJASRE.2022.8.11.3

Paired Sample T-Test for the measured modules Temperature

A paired sample t-test was conducted to evaluate the impact of dust accumulation on the surface of the solar module on temperature. Tables 6 and 7 present the result obtained from paired sample t-test in SPSS, there was a statistically significant decrease in temperature for the tracking module with (Mean = 44.25 ◦C, SD = 8.00) to the static module (Mean = 41.95 ◦C, SD = 7.31), r (209) t-value = 12.87, P<0.0005. The eta squared statistics, (0.44) indicate a large effect size. Therefore, we can conclude that there was a significant decrease in temperature when dust accumulates on the surface of the module from (Cohen 1988) eta value > 0.014 is considered a large effect.

4. RESULT OF CORRELATION ANALYSIS

In this section, we present all the result generated via the platform of SPSS version 2 with the applicable parameter of Table 8 utilized. The fairly large database created in excel was sorted and later transferred into the SPSS database. The relationship between the measured parameters from Table 8, were investigated using Pearson product-moment correlation coefficient, preliminary analyses were performed to ensure no violation of the assumptions of normality, linearity, and homoscedasticity. The outcome results are presented in Table 9. From this we reiterate that the main statistical results of significance as seen from closer inspection of results presented in Table 9, the foregoing emerged;

i. Highlighted cells indicate the variables that do not have a strong correlation with r < 0.4 and a P-value way below r < 0.05.
ii. The open circuit voltage (V_{OC}) does not appear correlated with the measured variables, therefore, was removed from the regression equation, since the dependent and independent variables being highly correlated is a requirement for regression analysis.
iii. Furthermore, the correlation between temperature and solar irradiance is very strong at (r = 0.82 and P-value < 0.005), and we should not have the two independent variables to be correlated with each other. Therefore, temperature is redundant, non- contributing variable and is excluded from the regression analysis.

Table 6: Paired Sample statistic

	Module Temperature Pair	
	(Tracking)	(Static)
Mean	44.25	41.95
Std. Deviation	8.00	7.31
Std. Error Mean	0.54	0.51
Significance	0.000	
Correlation	0.98	
N	210	

Table 7: Paired Sample Test from SPSS.

Module Temperature Paired Differences (Tracking) – (Static)	
Mean	2.30
Std. Deviation	0.69
Std. Error Mean	0.04
t - value	12.87
df	209
Sig. (2-tailed)	0.000

4.1 Result of Regression Analysis

Standard multiple regression was performed between the independent variables, dust weight (D), and the dependent variables; load power (P_L), load current (I_L), load voltage (V_L), short circuit current (I_{SC}) and open circuit voltage (V_{OC}). Analysis was performed using SPSS REGRESSION.

DOI: 10.31695/IJASRE.2022.8.11.3

Table 8: Pearson Product-Moment Between the Measured Variables

	Power	Irrad.	Dust	V_L	I_L	V_{OC}	I_{SC}	Temp
Power	1							
Irrad.	0.64	1						
Dust	0.69	**0**	1					
V_L	0.92	0.67	0.66	1				
I_L	0.98	0.61	0.73	0.88	1			
V_{OC}	**0.08**	**0.24**	**0.12**	**0.13**	**0.08**	1		
I_{SC}	0.98	0.54	0.79	0.90	0.98	0.05	1	
Temp	0.54	0.82	**0.01**	0.55	0.52	**0.17**	0.45	1

Table 9 displays the regression coefficients and the intercepts. Table 10 depicts the model summary including details of the F-test, p-values, standard error of the estimates, the significance of the test, and R^2**.** The obtained linear regression plots of P_L, I_L, V_L, V_{OC} and I_{SC} as a function of dust are shown in Figure 11 to 15, the relationship between P_L, I_L, V_L, V_{OC}, I_{SC} ($\%_{LOSS}$) with the measured dust weight is linear as revealed in Figures 11 to 16.

Table 9: Regression Coefficients of the Independent Variable Dust

	Coefficients		
Module Parameter	Intercept	Dust (D)	R^2
P_L	53.86	-0.97	0.9
V_L	15.45	-1.66	0.9
I_L	2.52	-0.036	0.9
V_{OC}	20.11	0.003	0.1
I_{SC}	3.88	-0.07	0.9

Table 10: Regression Outputs

Regression Output	Module Parameter				
	P_L	V_L	I_L	I_{SC}	V_{OC}
R^2	0.9	0.9	0.9	0.9	0.1
Adjusted R^2	0.9	0.9	0.9	0.9	0.1
Std. Error of Estimate	4.12	1.01	0.174	0.32	0.154
F-test	305	149	246	276	2.0
P-value	0.000	0.000	0.000	0.000	0.167

Figures 12 to 17 depict plots of module parameters in relation to dust. They are all shown to be linearly related to dust

DOI: 10.31695/IJASRE.2022.8.11.3

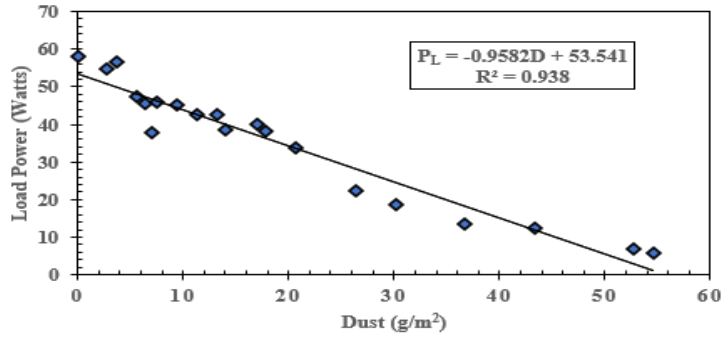

Figure 12: Plot of Module Load Power P_L Versus Dust Weight (D)

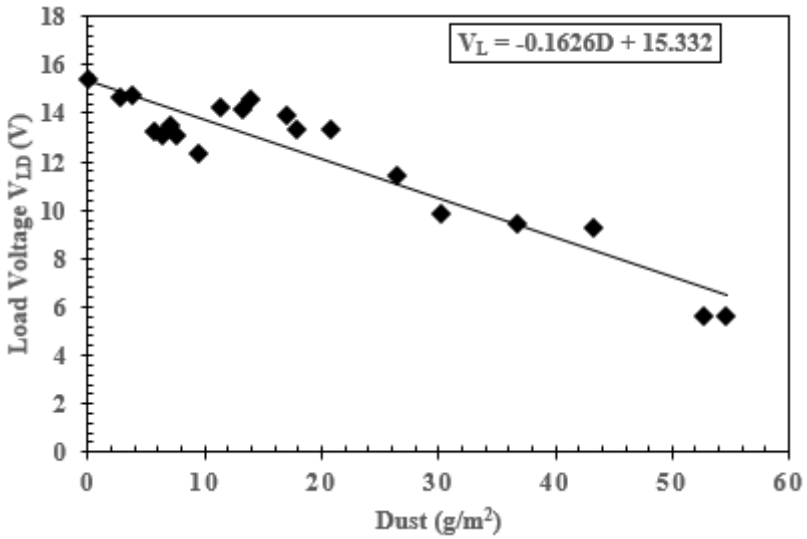

Figure 13: Plot of Module Load Voltage V_L Versus Dust Weight (D)

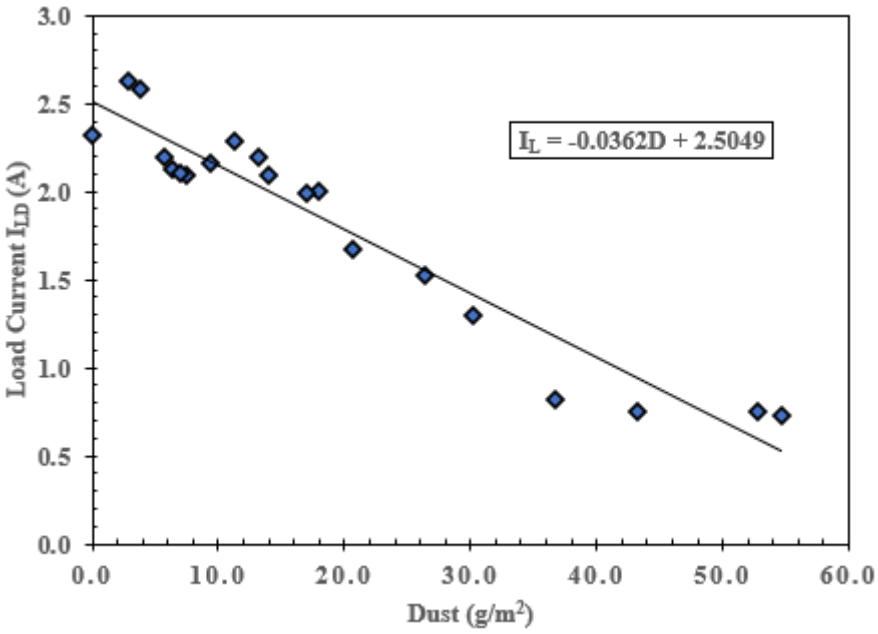

Figure 14: Plot of Module Load Current I_L Versus Dust Weight (D)

DOI: 10.31695/IJASRE.2022.8.11.3

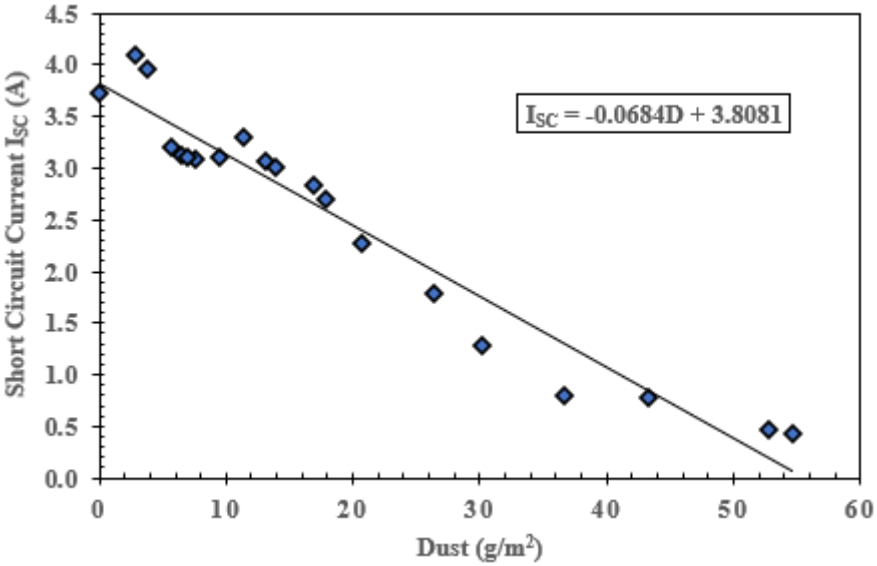

Figure 15: Plot of Short Circuit Current I_{SC} Versus Dust Weight (D)

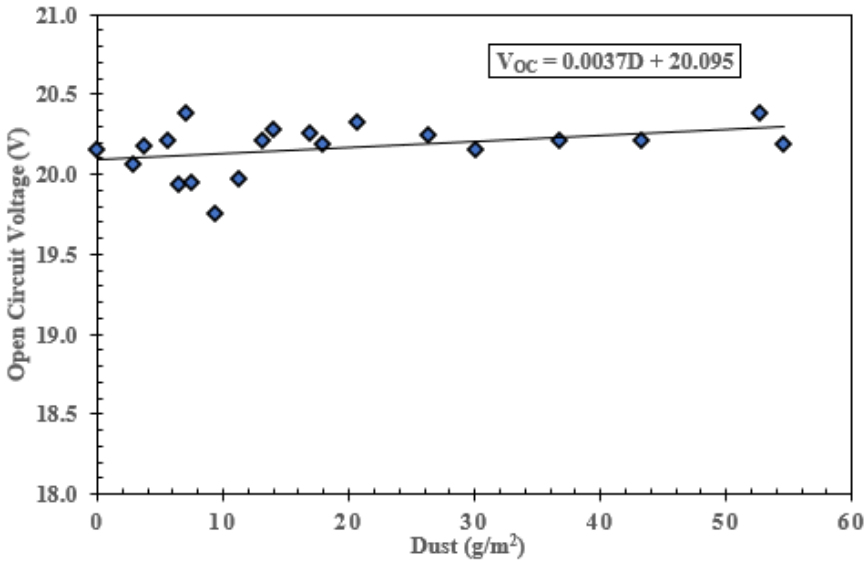

Figure 16: Plot of Open Circuit Voltage V_{OC} Versus Dust Weight (D)

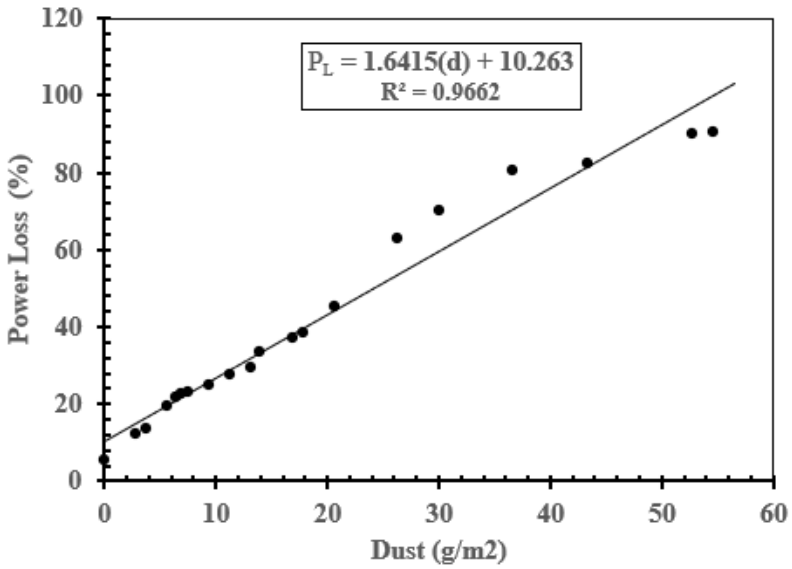

Figure 17: Plot of Percentage of Power Loss Versus Dust weight (D)

DOI: 10.31695/IJASRE.2022.8.11.3

The fitted linear empirical relationship for the experimental measurements on PV module as a function of dust are summarized in Table 11.

Table 11: Fitted Linear Empirical Relationship for the Experimental Measurements on PV Module

Module parameter	R^2	Empirical Equations	Dust Coefficient
P_L	0.9	$P_L = 53.8585 - 0.9679D$	$0.9679W/(g/m^2)$
V_L	0.9	$V_L = 15.4509 - 0.1663D$	0.1663W/(g/m2)
I_L	0.9	$I_L = 2.5248 - 0.0368D$	0.0368W/(g/m2)
I_{SC}	0.9	$I_{SC} = 3.8765 - 0.0706D$	0.0706W/(g/m2)
V_{OC}	0.1	$V_{OC} = 20.1177 - 0.0029D$	0.0029W/(g/m2)

4.2 Dust Sensitivity Coefficient for PV Module Parameters

As earlier observed, all PV module parameters have been established to be linearly related to dust as shown in Figures 12 to 17. Note that, the coefficient of fit (R^2) for each regression analysis is greater than (0.9). Interpretation of the result reveals some percentage drop or rise of each parameter for every (g/m^2) increase in dust. The following are the sensitivities of P_L, I_L, V_L, V_{OC} and I_{SC} with respect to dust.

- For 1 g/m^2 increase in dust weight P_L drops by1.83%
- For 1 g/m^2 increase in dust weight V_L drops by1.09%
- For 1 g/m^2 increase in dust weight I_L drops by 1.45%
- For 1 g/m^2 increase in dust weight drops I_{SC} by 1.84%
- For 1 g/m^2 increase in dust weight V_{OC} increases by 0.015%

These sensitivities coefficient apply to the polycrystalline silicon PV module investigated.

5. CONCLUSION

This paper investigated the impact of dust deposit on two scenarios of solar panel installation, that is, static (stationary) and tracking (single-axis movement) using field measurement, simulation and mathematical modeling technique (SPSS). Dust deposit was found out to be greater on a static solar panel than on a tracking PV module. The dust sensitivity coefficients further give the expected impact of every 1 g/m^2 increase in dust on the module's parameters which will help to predict the amount of dust deposit during the period under review in Bauchi metropolis, Nigeria, but with possibility for adaption to other locations with similar climatic conditions. This will aid in taking necessary measures to improve the performance of the module in the location, especially during that period of the year.

ACKNOWLEDGEMENT

This work is a part of an ongoing research funded by the Tertiary Education Trust Fund (TETFund) through Institution-Based Research (IBR) scheme.

REFERENCES

[1] S. O. Oyedepo, O. P. Babalola, S. C. Nwanya, O. Kilanko, R. O. Leramo, A. K. Aworinde, T. Adekeye, J. A. Oyebanji, A. O. Abidakun and O. L. Agberegha, "Towards a Sustainable Electricity Supply in Nigeria: The Role of Decentralized Renewable Energy System," *European Journal of Sustainable Development Research,* vol. 2, no. 4, pp. 1-31, 2018.

[2] P. Messerli and E. Muminingtyas, "The Future is now: Science for Achieving Sustainable Development," United Nation's Department of Economic and Social Affairs, 2019.

[3] The White House, "Building Resilient Supply Chains, Revitalizing, and Fostering Broad-Based Growth," The White House, Washington, 2021.

[4] The United Nations, "Technology and Innovation Report 2021 - Catching Technological Waves Innovation with

DOI: 10.31695/IJASRE.2022.8.11.3

Equity," United Nations, New York, U.S.A, 2021.

[5] T. Stamatelos and E. Roumpakias, "Surface Dust and Aerosol Effects on the Performance of Grid-Connected Photovoltaic Systems," *Journal of Sustainability,* vol. 12, no. 569, pp. 1-18, 2020.

[6] W. C. Solomon, N. Achara, D. K. Garba, S. U. Mohammed, N. C. A. Ozoekwe and H. Onyenweuwa, "Photovoltaic Maximum Power Point Dependency on Geographical Location," *American Journal of Engineering Research,* vol. 10, no. 7, pp. 119-125, 2021.

[7] A. J. Hamad, "Performance Evaluation of Polycrystalline Photovoltaic Module Based on Varying Temperature for Baghdad City Climate," *Journal of Advanced Research in Fluid Mechanics and Thermal Sciences,* vol. 67, no. 2, pp. 164-176, 2020.

[8] S. C. S. Costa, A. S. A. C. Diniz and L. L. Kazmerski, "Solar Energy Dust and Soiling R&D Progress: Literature Review Update for 2016," *Renewable and Sustainable Energy Reviews,* vol. 82, no. 3, pp. 2504-2536, 2017.

[9] P. G. Kosmopoulos, S. Kazadzis, M. Taylor, E. Athanasopoulou, O. Speyer, P. I. Raptis, E. Marinou, E. Proestakis, S. Solomos, E. Gerasopoulos, V. Amiridis, A. Bais and C. Kontoes, "Dust Impact on Surface Solar Irradiance Assessed with Model Simulations, Satellite Observations and Ground-Based Measurements," *Atmospheric Measuremnt Techniques,* vol. 10, pp. 2435-2453, 2017.

[10] M. Duranay, A. Turmus and V. Tanyildizi, "Experimental Efficiency Analysis of a Solar Panel Electricity Generation System using Planar Reflection," *The Institute of Engineering Technology Renewable Power Generation,* vol. 15, pp. 521-531, 2021.

DOI: 10.31695/IJASRE.2022.8.11.3